Manipulating Bandwidth of Cryogenically Cooled Receive-Only MRI Detectors

Zhurbenko, Vitaliy; Wang, Wenjun; Heredia, Juan Diego Sanchez; Ardenkjær-Larsen, Jan Henrik

Published in:
IEEE Sensors Letters

Link to article, DOI:
10.1109/LSENS.2023.3263972

Publication date:
2023

Document Version
Peer reviewed version

IEEE Sensors Letters Volume 7, No 4, 2023
Sensor Interface Circuits

Manipulating Bandwidth of Cryogenically Cooled Receive-only MRI Detectors

Vitaliy Zhurbenko, Wenjun Wang, Juan Diego Sanchez Heredia, Jan Henrik Ardenkjær-Larsen
Technical University of Denmark, Kgs. Lyngby, Denmark

Received 16-Feb-2023, revised 21-Mar-2023, accepted 28-Mar-2023.

Abstract—Cryogenically cooled MRI coils demonstrate extremely high *Q*-factors leading to a very narrow bandwidth. This bandwidth can be increased in a controlled manner using a preamplifier decoupling. In this work, an MRI coil design procedure is explained and an example showing over 2 times bandwidth increase in a cryogenic coil for 13C isotope imaging in 3-tesla MRI systems is demonstrated. The achieved wider bandwidth preserves the spectral components of magnetic resonance signals and makes coils less susceptive to detuning due to parasitic coupling to surrounding structures. The presented method is also useful in other applications of high-*Q* coils, for instance, in low field magnetic resonance imaging systems.

Index Terms—Coils, cryogenic electronics, high-Q coils, magnetic resonance imaging detectors, noise figure, noise matching, preamplifier decoupling.

I. INTRODUCTION

Cryogenic cooling is an efficient way of minimizing the thermal noise of magnetic resonance (MR) coils leading to a better signal-to-noise ratio (SNR) and MR image quality [1], [2]. This method is particularly beneficial when the noise induced by the presence of a lossy sample (e.g., animal, or human body) is considerably lower than the thermal noise from the conductive loss of the coil wire.

Due to reduced resistance, the *Q*-quality factor of the cooled coil increases considerably reducing the overall bandwidth of the imaging system. In such cases, the bandwidth sometimes becomes narrower than the acquired signal and might distort the spectrum of the magnetic resonance imaging (MRI) signal. A significant practical challenge is that the high-*Q* coils are very sensitive to the environment and are easily detuned in the presence of other coils and conductive parts of the scanner.

Preamplifier decoupling can be used to spoil the *Q*-factor of the receiver coil [3], [4]. In this work we demonstrate, that a small fraction of the preamplifier noise figure can be traded for further increase in bandwidth. In Fig.1 an example of SNR bandwidth manipulation using preamplifier decoupling in 13C, 3T cryogenic coils is shown and compared to a conventional power-matching approach.

Power-matching to 50 Ω (black curve in Fig.1) exhibits narrowest bandwidth, which might present a challenge in some imaging applications. On the other hand, inductive loops using preamplifier decoupling [4] are interfaced with a relatively large resistance [3], which effectively reduces the *Q*-factor of the coil leading to a wider bandwidth. This can be observed comparing to a blue curve in Fig.1, representing SNR in a preamplifier decoupled coil with a traditional matching for the minimum noise figure F_{min} of the preamplifier.

In the following Section it is shown how to further increase the bandwidth of the coil sacrificing the noise figure of the preamplifier in a controlled manner.

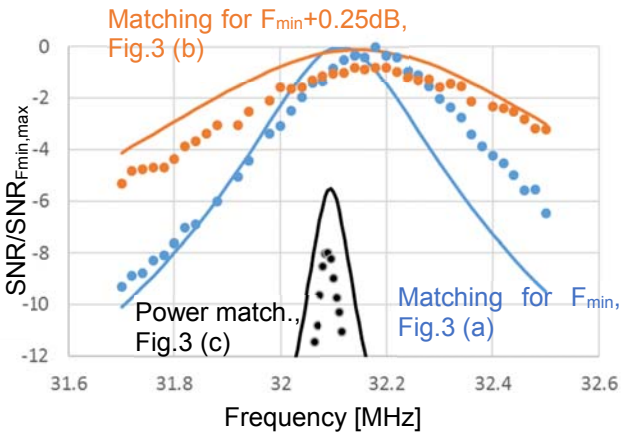

Fig. 1. Solid curves – simulated, dots – measured normalized SNR frequency sweep for coils in Fig.3, Fig.4 using power matching and preamplifier decoupled noise matching. Widest SNR bandwidth is achieved with preamplifier decoupling matched for F_{min}+0.25dB.

The orange curve in Fig.1 demonstrates over 2 times increase in bandwidth if the circuit is designed for noise figure 0.25dB higher than F_{min}.

II. METHODS

In the considered here setup, the coil is connected to a low noise preamplifier through a circuit, which transforms input impedance of the preamplifier Z_a to a large impedance appearing at the terminals of the coil. This circuit is typically designed to transform the coil impedance Z_{coil} to the optimal noise impedance of the preamplifier $Z_{n,opt}$, shown as a blue dot on the Smith Chart in Fig.2.

Corresponding author: Vitaliy Zhurbenko (vizh@dtu.dk).

Digital Object Identifier: 10.1109/LSEN.2023.3263972.

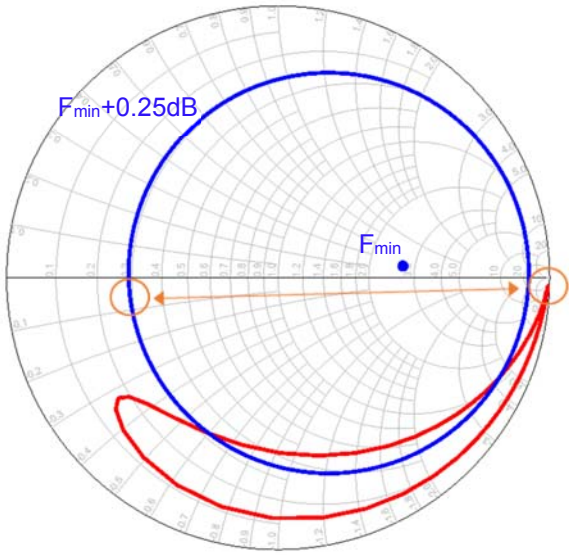

Fig. 2. Smith chart. Blue dot – optimal noise impedance of the preamplifier for F_{min}, $Z_{n,opt}$≈134+j15 Ω. Blue circle – noise figure circle of the preamp for F_{min}+0.25dB. Red curve - power reflection coefficient of the preamp relative to the source impedance on the noise figure circle: $\Gamma_a=(Z_a-Z^*_{n,Fmin+0.25dB})/(Z_a+Z_{n,Fmin+0.25dB})$. Maximum magnitude of the reflection coefficient corresponds to source impedance $Z_{n,Fmin+0.25dB}$≈15-j5 Ω (indicated by the orange circle on the left).

This unique impedance, together with the given Z_a, and Z_{coil}, unambiguously defines the impedance presented to the terminals of the coil [4], and consequently, the degree of spoiling the coil *Q*-factor.

On the other hand, matching to a higher noise figure, for example F_{min}+0.25dB, results in an infinite range of source impedances $Z_{n,Fmin+0.25dB}$, shown on the blue noise figure circle in Fig.2. Out of this infinite range we can choose the source impedance $Z_{n,Fmin+0.25dB}$, which leads to the highest magnitude of the power reflection coefficient [4] at the preamplifier input. This will lead to even higher impedance at the terminals of the coil further spoiling the coil *Q*-factor, which facilitates further bandwidth increase.

III. PROCEDURES AND RESULTS

To demonstrate the concept, this matching network design approach is implemented and compared to a traditional preamplifier decoupling and power matching (implemented designs are shown in Fig.3). Since cryogenic cooling is typically used in cases when coil noise is dominating, in this demonstration the sample noise is neglected and the measurements here are thus conducted without a sample loading. The coil loop is 8 cm in diameter made of ⌀2 mm copper wire (photographs are shown in Fig.4). Using the equations for wire loop impedance [5] and assuming the conductivity of copper at 77K is 10^9/3.5 S/m, the calculated Z_{coil} at 32.1 MHz is indicated in Fig.3. For the implemented preamplifier [6] without power protection diodes Z_a≈144-j844 Ω. The circuit elements are calculated using design equations (21), (22) published in [4] and Z_a, Z_{coil} from Fig.3, and $Z_{n,opt}$ (or $Z_{n,Fmin+0.25dB}$) from Fig.2.

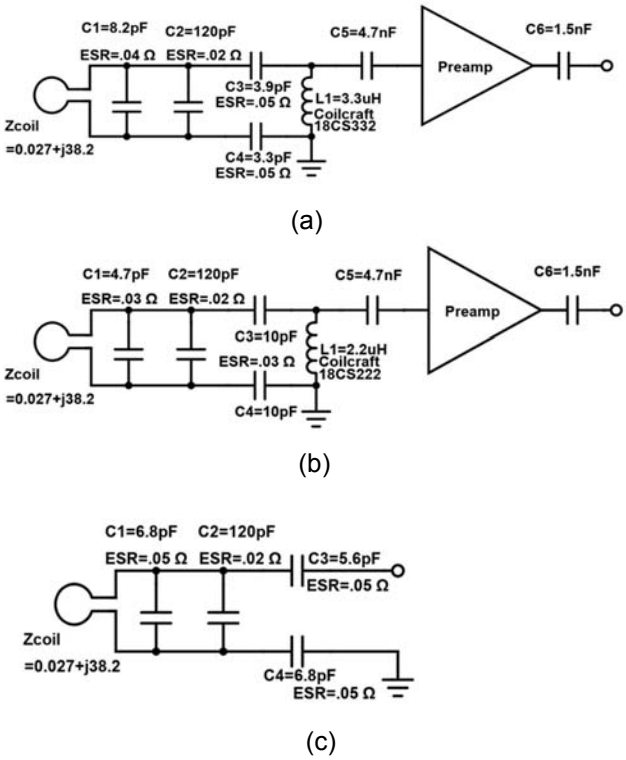

Fig. 3. Circuit diagram of the matching network for (a) preamplifier decoupled coil matched for F_{min}; (b) preamplifier decoupled coil matched for F_{min}+0.25 dB; (c) power (complex conjugated) matched coil to 50 Ω.

Out of 4 possible solutions for matching networks, a Π-network topology is chosen for implementation.

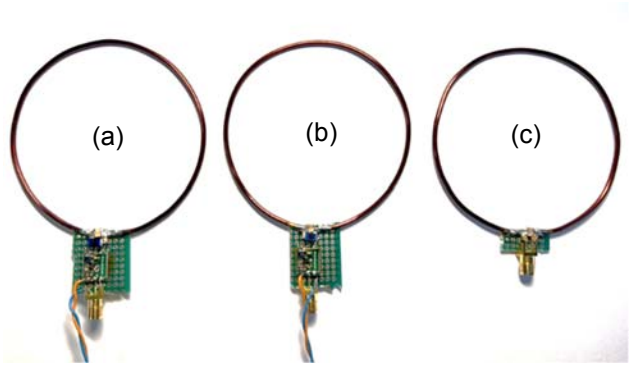

Fig. 4. Photograph of the fabricated cryogenic coils. (a) preamplifier decoupled coil matched for Fmin; (b) preamplifier decoupled coil matched for Fmin+0.25dB; (c) power (complex conjugated) matched coil to 50Ω.

Series capacitors are split into C_3 and C_4 for symmetry and the capacitor next to the coil is realized as a parallel combination of C_1 and C_2 to achieve accurate tuning, as shown in Fig.3. Capacitors C_5

and C_6 are for DC-decoupling, 0604 form-factor and supposed to have a negligible influence on the detector function.

The form-factor of the implemented tuning capacitors C_1 …C_4 is 1111. Since the losses of the capacitors may be comparable to the resistance of the cryogenic coil, their equivalent-self-resistance (ESR) is extracted from the datasheet and is indicated in Fig.3. It was not possible to identify the significance of the resistance of soldering at cryogenic temperatures. This resistance was therefore omitted in the circuit model. The circuits in Fig. 3 are simulated using a commercial circuit simulator. The simulation results are shown in Fig.1. The simulated 0.1 dB SNR bandwidth of the power matched cryogenic coil in Fig. 4(c), Fig. 3(c) is approximately 10 kHz. It is extended to ≈ 42 kHz using the traditional preamplifier decoupling with matching for F_{min} (Fig. 4(a), Fig. 3(a)), and is further extended to 114 kHz by matching for F_{min}+0.25 dB. In theory, there supposed to be 0.25 dB difference between the peaks of the simulated SNR blue curve (F_{min}) and orange curve (F_{min}+0.25 dB). This difference is however slightly lower since the capacitors and the inductors have loss, while the design equations in [4] are for lossless components.

The SNR measurement setup is schematically illustrated in Fig.5.

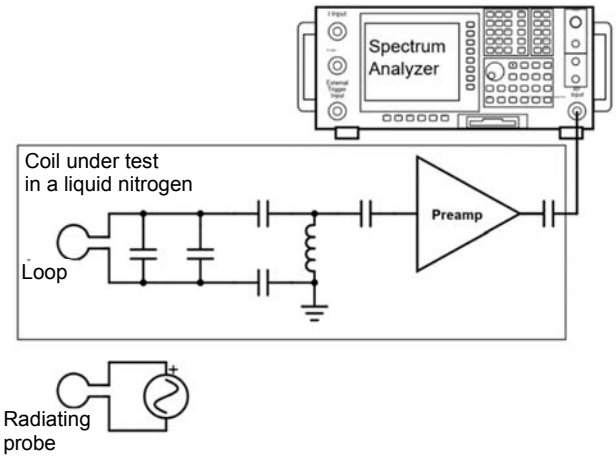

Fig. 5. Schematic representation of the SNR measurement setup. Signal from the subject is modelled by a radiating shielded loop probe connected to a signal generator. Signal and the noise are measured by a spectrum analyzer Agilent E4440A. The measured data is stored and plotted on a computer.

During the test, the coil is connected to a spectrum analyzer, which records total noise and the signal picked up from the radiating loop probe. The measurement results from this design example are plotted in Fig. 1 next to the simulation results.

IV. DISCUSSION AND CONCLUSION

The measured SNR sweep in Fig.1 follows the simulations with the achieved bandwidth of approximately 8.4 kHz, 47 kHz, and 112 kHz for the cases in Fig.3(c), (a), and (b) respectively. The SNR of the passive power-matched coil (the black curve in Fig. 1) is lower because, according to Friis equation [7], the noise figure of the spectrum analyzer degrades the SNR of the receiver. This noise figure is set to 5.5 dB [8] in the simulations. The gain of the preamplifiers removes the influence of the noise figure of the spectrum analyzer almost entirely and therefore the SNR of the preamplifier decoupled coils appears higher (orange and blue curves in Fig.1).

The presented design approach demonstrates the increase in bandwidth, which makes the MRI detectors less prone to detuning due to interaction with the environment. It could be mentioned that in the case when the sample loading can not be neglected, the loading will further contribute to broadening the bandwidth of the coil. Thus, as long as the total loss is coil dominated, the proposed approach can be used to control the bandwidth of the coil.

REFERENCES

[1] Darrasse L, Ginefri JC. “Perspectives with cryogenic RF probes in biomedical MRI,” *Biochimie*. 2003, 85, pp.915-937.

[2] Wenjun Wang, Juan Diego Sánchez-Heredia, Rie Beck Olin, Esben Søvsø Szocska Hansen, Christoffer Laustsen, Vitaliy Zhurbenko, Jan Henrik Ardenkjær-Larsen, “A cryogenic fourteen-channel 13C receiver array for 3 T human head imaging,” *Magnetic Resonance in Medicine*, Volume 89, Issue 3, March 2023, pp. 1265-1277.

[3] Roemer PB, Edelstein WA, Hayes CE, Souza SP, Mueller OM. ”The NMR phased array,” *Magnetic Resonance in Medicine* 1990, 16, pp.192-225.

[4] Wenjun Wang, Vitaliy Zhurbenko, Juan Diego Sánchez-Heredia, Jan. H. Ardenkjær-Larsen, “Trade-off between preamplifier noise figure and decoupling in MRI detectors,” *Magnetic Resonance in Medicine*, Volume 89, Issue 2, October 2022, pp. 859-871.

[5] Wenjun Wang, Juan Diego Sánchez Heredia, Vitaliy Zhurbenko, and Jan Henrik Ardenkjær Larsen, “Condition for optimal preamplifier decoupling in one-turn single- and multi-gap shielded loop MRI detectors,” in *Proceedings of IEEE 2nd Ukrainian Microwave Week*, online, Kharkiv, Ukraine, November, 2022, pp. 150-154.

[6] LNA, elcry1-ln datasheet. Available online: elcry.com.

[7] H. T. Friis, "Noise Figures of Radio Receivers," in *Proceedings of the IRE*, vol. 32, no. 7, pp. 419-422, July 1944.

[8] Agilent Technologies PSA Series Spectrum Analyzers Specifications Guide. July 2012. Agilent Technologies, USA.